Int J Adv Manuf Technol (2016) 85:149–156
DOI 10.1007/s00170-015-7789-4

ORIGINAL ARTICLE

Comprehensive error measurement and compensation method for equivalent cutting forces

Xianli Shi[1] · **Huanlao Liu**[1] · **Hao Li**[1] · **Can Liu**[1] · **Guangyu Tan**[1]

Received: 23 April 2015 / Accepted: 31 August 2015 / Published online: 9 October 2015

Abstract To determine the error compensation for cutting forces with a machine tool, this paper proposes a comprehensive error compensation method that determines an equivalent cutting force. The loading system that applies this equivalent cutting force was designed to load a constant force that imitates the actual cutting force of a machine tool. The equivalent cutting force, when applied to the working table of the machine tool, induces an error that can be directly measured by a laser interferometer. Moreover, a stable measurement environment suitable for laser interferometer is configured. A comprehensive error compensation model of a three-axis computer numerical control (CNC) machine tool was developed using multi-body systems theory and homogeneous transformation matrices. Solutions for the error compensation model and parametric equation were automatically found using MATLAB, based on this model. The effectiveness of this compensation method has been confirmed by machining experiments. The experimental results show that this comprehensive error compensation of the equivalent cutting force can greatly improve machining accuracy.

Keywords Equivalent cutting force · Cutting-force-induced error · Comprehensive error measurement · Software error compensation

✉ Huanlao Liu
huanlao_liu@hotmail.com; hl66@163.com

[1] College of Engineering, Guangdong Ocean University, Zhanjiang, Guangdong 524000, People's Republic of China

1 Introduction

The demand on modern manufacturing industries is for greater accuracy in product fabrication and higher stability in quality. The most important factor of the precision components is the accuracy of the machine tools. Mainly, position errors are originated from geometric, thermal, cutting force, dynamic loading, etc. [1, 2]. Many researchers have developed the geometric error thermal error measurement methods and models. Ramesh et al. [1] analyzed various sources of geometric errors that were usually encountered on machine tools. Liu et al. [3] investigated the various characteristics of geometric errors, such as position dependence, relative positioning, synthesis, and continuity; a relay method was proposed by which the geometric error can be measured over the whole workspace. To determine the geometric errors relevant for the manufacturing and installation of machine tool parts, Tian et al. [4] proposed a general error modeling approach. Zhu et al. [5] used rigid-body kinematics to complete error modeling for computer numerical control (CNC) machine tools, using laser interferometers and ball-bars to successfully identify the geometric-error parameters. Srivastava et al. [6] proposed a universal comprehensive compensation scheme to offset geometric and thermal errors by analyzing the structure of kinematic machine tools, which are mainly used in specific types of machine tools; the universality of this method needs to be further improved. Aha et al. [7] included backlash error to a volumetric error model. Lin [8] proposed a new matrix summation method for geometric-error compensation, but integrating this compensation method in applications is cumbersome. Belforte et al. [9] developed a self-calibration model that depends on 18 error parameters. The reduced-order Legendre polynomials are used to model and identify these 18 functions, but this method cannot accurately compensate perpendicularity errors. Using the Jacobian–Torsor theory, Zuo

et al. [10] determined the geometric-error parameters of each rigid body; manufacturing product errors were accurately predicted and compensated. Jung et al. [11] used a parameterized error model to analyze machine tool errors within the workspace and the methodology of on-machine measurement for improving the machining accuracy. Based on the rigid-body kinematics, positioning errors derived using the homogeneous transformation matrices are parameterized by approximating error components with polynomial functions.

The other major cause of inaccuracy in CNC machine tools is error due to cutting force because the hard cutting and hard cutting material are used widely recently. Engin et al. [12] developed a general error compensation model; this method uses a piezoelectric dynamometer to measure the average cutting forces. Raksiri et al. [13] proposed the off-line error compensation scheme on a three-axis CNC machine tool that implements an evaluation of the cutting-force-induced errors using the BP neural network. For machining thin-walled work pieces, Ratchev et al. [14] developed a multiple error compensation algorithm. Applying gene expression programming, Yang et al. [15] performed numerical calculations of milling forces, showing that when compared with other methods, the degree of measurement data fitting obtained by this method is highly correlated with experimental measurement data. Schmitz et al. [16] performed a series of studies on milling force error by comparing milling errors of the work piece and the measurement results of a plane grating. For end-milling machined work pieces with concave and convex curved surfaces, Ikua et al. [17] proposed a theoretical model to predict the cutting force and machining error. Chen et al. [18] modeled cutting-force-induced errors based on the theory of fuzzy neural network systems and current signals, using Hall current sensors to indirectly measure cutting forces. A real-time compensation system for the cutting-force-induced error was proposed.

Previous researches on comprehensive compensation of both geometric and cutting-force-induced errors have mainly been on obtaining separate compensations for the two types of errors. The corresponding relationship between force and error is then indirectly established using certain technical methods. This paper is organized into four sections. The first section mainly discusses the measurement method of the equivalent cutting-force-induced error by the laser interferometer. Using the equivalent cutting force to simulate the actual cutting force in machine tool, the setup has been established to identify the error parameters along the X and Y-axes. The second section discusses the combination of geometric model under the condition of equivalent cutting force. This comprehensive error model is developed by multi-body systems theory and homogeneous transformation metrics, which include a total of 18 error components. It is used to compensate both geometric and cutting-force-induced errors simultaneously. The third section discusses the compensation results. A special designed experimental test is carried out in order to validate the performance under three different errors compensation. The conclusions are given in the final section.

2 Mechanism of equivalent cutting

2.1 Measurement of equivalent cutting force

The equivalent cutting force is determined from the measurement of actual cutting forces, which simulate the actual cutting force along the X- and Y-axes of the machine tool in a particular manner. Considering the limitations in the current experimental setup, the cutting-force-induced error along the Z-axis will not be studied. The error associated with the equivalent cutting force is called the equivalent cutting-force-induced error.

To measure the magnitude of the milling force under different processing conditions, a carbide tool CYT ME550, 45 steel, a XH714 CNC milling machine, and a SDC-C4F universal dynamometer were used in the tests. This paper adopts the orthogonal test to perform data measurements. The orthogonal test can acquire comprehensive test information when the limited experimental data is used. The main factors affecting the cutting force are cutting width, cutting depth, spindle speed, and feed. This study sets up four groups of different cutting parameters. These are listed in Table 1.

The measurement device of the actual milling force is shown in Fig. 1. The SDC-C4F universal dynamometer has different data sampling frequency, so different sampling frequency was taken according to the cutting speed. The measurement results of the cutting force are shown in Table 2.

Considering actual cutting parameter for the validity experimental tests (in section 4), the seventh group of experimental data in Table 2 is chosen as the reference standard of the equivalent cutting force. Hence, it avoids the negative effects on the compensation results that derive from an unreasonable choice of an equivalent cutting force. The equivalent cutting forces along the X- and Y-axes were set to 110 and 180 N.

Table 1 Cutting parameters

Cutting parameters	1#	2#	3#	4#
Speed n (rpm)	1240	3350	4480	6270
Cutting depth a_p (mm)	0.4	0.6	0.8	1
Cutting width a_e(mm)	1	3	5	7
Feed f (mm)	0.2	0.4	0.6	0.8

Fig. 1 the setup of milling force measuring experiment

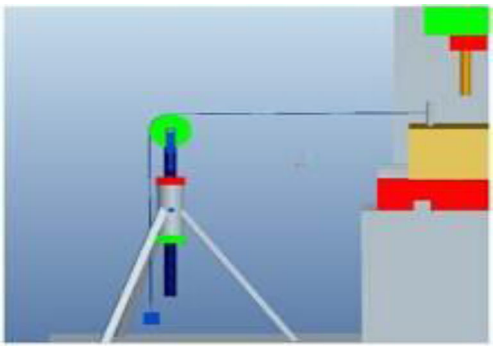

Fig. 2 Schematic illustrating equivalent cutting force loading

2.2 Error measuring system of the equivalent milling force

After the equivalent milling force is selected, this force is then applied to the work table of the machine tool using a pulley mechanism, wire rope, and tripod (Fig. 2). Hence, the weight moves vertically around the pulley as the work table of the machine tool moves horizontally finally, and the actual milling force will be simulated by this way. The feed speed (not too fast or too slow) should be properly selected which should not be caused vibration of the machine table. The error measuring system of the equivalent milling force can be stabilized. This setup provides ideal conditions to use laser interferometer under the stress state of machine tool. The schematic illustrating equivalent cutting-force loading is shown in Fig. 2, and the setup for field measurements of the error parameters is shown in Fig. 3.

3 Error model under the condition of equivalent cutting force

A mathematical model determining comprehensive error compensation has been developed that uses homogeneous coordinate transformations and rigid-body kinematics. During the application of the equivalent cutting force, the measurement results for the X- and Y-axis directions from laser interferometer are the coupling value about the geometrical and cutting-force-induced error. The coupled parameters are referred to as the comprehensive error parameters (Table 3). There are in total 21 error components for three-axis milling machine, which is supposed that the angle errors between the axes are small, so 18 errors components have been considered. Here, subscript e refers to the equivalent cutting force, and subscripts x, y, and z refer to the error direction or the rotation axis of the error direction. The X, Y, and Z in parentheses represent the direction of motion.

Table 2 Measurement results for the milling force using the orthogonal test

Test group	Cutting depth a_p (mm)	Amount of feed per tooth f_z (mm)	Cutting width a_e (mm/min)	Feed speed F (mm/min)	Sampling frequency f_s	Fxmax F_{xmax} (N)	Fymax F_{xmax} (N)
1#	0.4	0.2	1	205	3270	65.03	81.35
2#	0.4	0.4	3	750	7340	78.35	189.64
3#	0.4	0.6	5	1408	11530	161.25	194.65
4#	0.4	0.8	7	2496	14930	154.69	153.64
5#	0.6	0.6	3	415	3270	103.97	306.54
6#	0.6	0.8	1	1270	7340	123.35	182.49
7#	0.6	0.2	7	750	11530	102.00	186.32
8#	0.6	0.4	5	1530	14930	154.50	179.39
9#	0.8	0.8	5	540	3270	138.67	310.56
10#	0.8	0.6	7	1200	7340	320.30	411.58
11#	0.8	0.4	1	1080	11530	253.21	151.36
12#	0.8	0.2	3	960	14930	152.62	203.65
13#	1.0	0.4	7	310	3270	148.60	349.54
14#	1.0	0.2	5	540	7340	330.10	336.89
15#	1.0	0.8	3	1810	11530	346.62	302.53
16#	1.0	0.6	1	2030	14930	226.50	206.67

Fig. 3 The measurements setup of error parameters

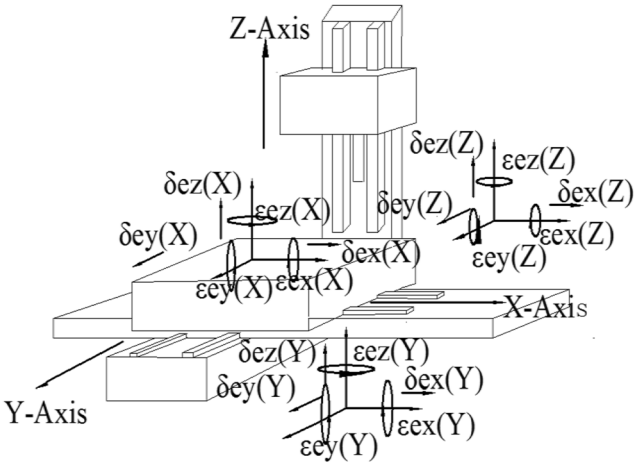

Fig. 4 Distribution of error parameters

Because of limitations in the experimental setup, the equivalent cutting force is unloaded along the Z-axis; the error component caused by the force to Z-axis will be ignored. The error parameter along the Z-axis is retaining generality. The measurement results comprise the geometric error and equivalent cutting-force error along the X- and Y-axis. However, the measurement results from laser interferometer will still be called the comprehensive error parameters. The error parameters of the machine tool spindle, work table, and Y-axis are depicted in Fig. 4.

3.1 Establishment of the coordinate system

The machine tool structure is divided into tool and work-piece branches under the action of the equivalent cutting force. To perform the equivalent transformation for the pose error of all the moving parts in each component, a series of coordinate systems needs to be established for each of the moving parts. The base coordinate system provides a reference for all other coordinate systems. To simplify such transformations, the base coordinate system is fixed on the machine tool bed. The X- and Y-axes of the base coordinate system are set parallel to the X and Y direction of the machine tool, respectively; the X-axes is located in the plane which is made up by the translation-pairs of reference axis along the X direction of machine tool and the Y-axis of the base coordinates. The right-hand screw rule determines the Z-axis, which forms a Cartesian coordinate system with the X- and Y-axes of the base coordinate system.

For the tool and work-piece branches, the actual moving reference coordinate system of the slide plate is superimposed with the ideal moving reference coordinate system. The actual motion reference coordinate system of the work table produces a perpendicularity error $\varepsilon_e xy$ relative to the body coordinate system of the Y-axis direction slide plate. The position vector of the work-piece body coordinate system is denoted $P_{ew}=(-P_{ewx}, P_{ewy}, P_{ewz}, 1)^T$ relative to the body coordinate system of the work table. For the bed-tool branch chain, the position vector of the ideal motion reference coordinate system of the spindle box is $P_{et}=(P_{etx}, P_{ety}, P_{etz}, 1)^T$ with respect to the bed-body coordinate system. The actual moving reference coordinate system produces perpendicularity errors $\varepsilon_e yz$ and $\varepsilon_e xz$ relative to the ideal kinematic reference coordinate system. Because there is no relative motion between the cutting tool and the spindle box, the error component is assumed to be zero.

3.2 Description of the characteristic matrix

The equivalent position error characteristic matrix $T_{ebs.pe}$, the equivalent position feature matrix $T_{ebs.p}$, the equivalent error motion characteristic matrix $T_{ebs.se}$, and the actual total

Table 3 Comprehensive error parameters

	Error in linear displacement	Error in angular displacement
X-axis error parameters	$\delta_{ex}(X)$, $\delta_{ey}(X)$, $\delta_{ez}(X)$	$\varepsilon_{ex}(X)$, $\varepsilon_{ey}(X)$, $\varepsilon_{ez}(X)$
Y-axis error parameters	$\delta_{ey}(Y)$, $\delta_{ex}(Y)$, $\delta_{ez}(Y)$	$\varepsilon_{ey}(Y)$, $\varepsilon_{ex}(Y)$, $\varepsilon_{ez}(Y)$
Z-axis error parameters	$\delta_{ez}(Z)$, $\delta_{ex}(Z)$, $\delta_{ey}(Z)$	$\varepsilon_{ez}(Z)$, $\varepsilon_{ex}(Z)$, $\varepsilon_{ey}(Z)$

equivalent characteristic matrix T_{ebs} between the machine tool bed and the slide plate of Y-axis direction are given as follows:

$$T_{ebs.pe} = T_{ebs.p} = \begin{bmatrix} 1 & 0 & 0 & 0 \\ 0 & 1 & 0 & 0 \\ 0 & 0 & 1 & 0 \\ 0 & 0 & 0 & 1 \end{bmatrix}, \quad T_{ebs.s} = \begin{bmatrix} 1 & 0 & 0 & 0 \\ 0 & 1 & 0 & y \\ 0 & 0 & 1 & 0 \\ 0 & 0 & 0 & 1 \end{bmatrix}$$
$$T_{ebs.se} = \begin{bmatrix} 1 & -\varepsilon_{es.sz} & \varepsilon_{es.sy}^{es.sy} & \delta_{es.sx} \\ \varepsilon_{es.sz} & 1 & -\varepsilon_{es.sx} & \delta_{es.sy} \\ -\varepsilon_{es.sy} & \varepsilon_{es.sx} & 1 & \delta_{es.sz} \\ 0 & 0 & 0 & 1 \end{bmatrix} \quad (1)$$
$$T_{ebs} = T_{ebs.p}.T_{ebs.pe}.T_{ebs.s}.T_{ebs.se}.$$

Similarly, the equivalent position error characteristic matrix $T_{est.pe}$, the equivalent position feature matrix $T_{est.p}$, the equivalent displacement error characteristic matrix $T_{est.se}$, the equivalent displacement characteristics matrix $T_{est.s}$, and the actual total equivalent characteristic matrix T_{est} between the working table and the Y-axis direction slide plate are as follows:

$$T_{est.se} = \begin{bmatrix} 1 & 0 & 0 & 0 \\ 0 & 1 & 0 & 0 \\ 0 & 0 & 1 & 0 \\ 0 & 0 & 0 & 1 \end{bmatrix}, T_{est.pe} = \begin{bmatrix} 1 & -\varepsilon_{exy} & 0 & 0 \\ \varepsilon_{exy} & 1 & 0 & 0 \\ 0 & 0 & 1 & 0 \\ 0 & 0 & 0 & 1 \end{bmatrix}, T_{est.s} = \begin{bmatrix} 1 & 0 & 0 & x \\ 0 & 1 & 0 & 0 \\ 0 & 0 & 1 & 0 \\ 0 & 0 & 0 & 1 \end{bmatrix},$$
$$T_{est.se} = \begin{bmatrix} 1 & -\varepsilon_{ew.sz} & \varepsilon_{ew.sy}^{ew.sy} & \delta_{ew.sx} \\ \varepsilon_{ew.sz} & 1 & -\varepsilon_{ew.sx} & \delta_{ew.sy} \\ -\varepsilon_{ew.sy} & \varepsilon_{ew.sx} & 1 & \delta_{ew.sz} \\ 0 & 0 & 0 & 1 \end{bmatrix}$$
$$T_{est} = T_{est.pe}.T_{est.pe}.T_{est.pe}.T_{est.se}. \quad (2)$$

Also, the equivalent position error characteristic matrix $T_{etw.pe}$, the equivalent position feature matrix $T_{etw.p}$, the equivalent displacement error characteristic matrix $T_{etw.se}$, the equivalent displacement characteristics matrix $T_{etw.s}$, and the actual total equivalent characteristic matrix T_{etw} between the working table and the work-piece are as follows:

$$T_{etw.p} = \begin{bmatrix} 1 & 0 & 0 & p_{ewx} \\ 0 & 1 & 0 & p_{ewy} \\ 0 & 0 & 1 & p_{ewz} \\ 0 & 0 & 0 & 1 \end{bmatrix},$$
$$T_{etw.pe} = T_{etw.s} = T_{etw.se} = \begin{bmatrix} 1 & 0 & 0 & 0 \\ 0 & 1 & 0 & 0 \\ 0 & 0 & 1 & 0 \\ 0 & 0 & 0 & 1 \end{bmatrix} \quad (3)$$
$$T_{etw} = T_{etw.p}.T_{etw.pe}.T_{etw.s}.T_{etw.se}\ .$$

Next, the equivalent position error characteristic matrix $T_{ebb.pe}$, the equivalent position feature matrix $T_{ebb.p}$, the equivalent displacement error characteristic matrix $T_{ebb.se}$, the equivalent displacement characteristics matrix $T_{ebb.s}$, and the actual total equivalent characteristic matrix T_{ebb} between the machine tool bed and the spindle box are as follows:

$$T_{ebb.p} = \begin{bmatrix} 1 & 0 & 0 & p_{esx} \\ 0 & 1 & 0 & p_{esy} \\ 0 & 0 & 1 & p_{esz} \\ 0 & 0 & 0 & 1 \end{bmatrix}, T_{ebb.pe} = \begin{bmatrix} 1 & 0 & \varepsilon_{exz} & 0 \\ 0 & 1 & -\varepsilon_{eyz} & 0 \\ -\varepsilon_{exz} & \varepsilon_{eyz} & 1 & 0 \\ 0 & 0 & 0 & 1 \end{bmatrix}$$
$$T_{ebb.s} = \begin{bmatrix} 1 & 0 & 0 & 0 \\ 0 & 1 & 0 & 0 \\ 0 & 0 & 1 & z \\ 0 & 0 & 0 & 1 \end{bmatrix} \quad (4)$$
$$T_{ebb.se} = \begin{bmatrix} 1 & -\varepsilon_{eb.sz} & \varepsilon_{eb.sy}^{eb.sy} & \delta_{eb.sx} \\ \varepsilon_{eb.sz} & 1 & -\varepsilon_{eb.sx} & \delta_{eb.sy} \\ -\varepsilon_{eb.sy} & \varepsilon_{eb.sx} & 1 & \delta_{eb.sz} \\ 0 & 0 & 0 & 1 \end{bmatrix}$$
$$T_{ebb} = T_{ebb.p}.T_{ebb.pe}.T_{ebb.s}T_{ebb.se}$$

Finally, the equivalent position error characteristic matrix $T_{ebt.pe}$, the equivalent position feature matrix $T_{ebt.p}$, the equivalent displacement error characteristic matrix $T_{ebt.se}$, the equivalent displacement characteristics matrix $T_{ebt.s}$, and the actual total equivalent characteristic matrix T_{ebt} between the machine tool cutter and the spindle box are as follows:

$$T_{ebt} = T_{ebt.p}.T_{ebt.pe}.T_{ebt.s}.T_{ebt.se} = I \quad (5)$$

3.3 Derivation of the comprehensive error compensate model

The coordinate value for the tool-tip point should coincide with the coordinate value from the processed point of the work-piece when these two points are transformed to the base coordinate system in the ideal case. However, in actuality, these coordinate values of two points are not same, and the difference between the two points is the machining error of the machine tool. It can be assumed that the coordinate value of the center point of the tool is $\boldsymbol{P_{etc}}=(x_{et},y_{et},z_{et},1)^T$ in the tool coordinate system. Moreover, the coordinate value of the point to be processed on the work-piece is assumed to be $\boldsymbol{P_{ewp}}=(x_{ewp},y_{ewp},z_{ewp},1)^T$ in the work-piece coordinate

Fig. 5 Milled work pieces under different error compensation scheme

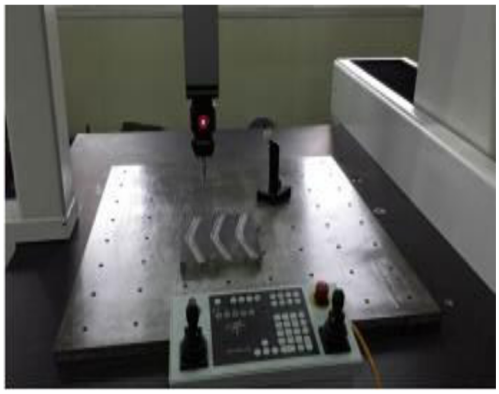

Fig. 6 Measurement experiment

system. The equivalent position vectors of the tool-tip point and the point to be processed are $\boldsymbol{P_{etb}}$ and $\boldsymbol{P_{ewb}}$, respectively.

$$P_{etb} = T_{ebb.p}.T_{ebb.pe}.T_{ebb.s}.T_{ebb.se}, .T_{ebt.p}.T_{ebt.pe}.T_{ebt.s}.T_{ebt.se}.P_{etc} \quad (6)$$

$$P_{ewb} = T_{ebs.p}.T_{ebs.pe}.T_{ebs.s}T_{ebs.se}T_{est.p}.T_{est.pe}. T_{est.s}.T_{est.se}.T_{etw.p}.T_{etw.pe}.T_{etw.s}.T_{etw.se}.P_{ewp} \quad (7)$$

The equivalent pose error $\boldsymbol{E_e}$ between the tool-tip point and the point to be processed in the work-piece is shown as follows:

$$E_e = P_{etb} - P_{ewb} \quad (8)$$

Equation (8) represents the comprehensive error compensation model for the three-axis CNC machine tool. The comprehensive error parameters are identified by laser interferometer and the nine-line method. Because the equivalent cutting force acts along both the X- and Y-axis directions, the comprehensive error value will be the algebraic sum of the geometric error and force error. Hence, this method does not require an independent measurement of both.

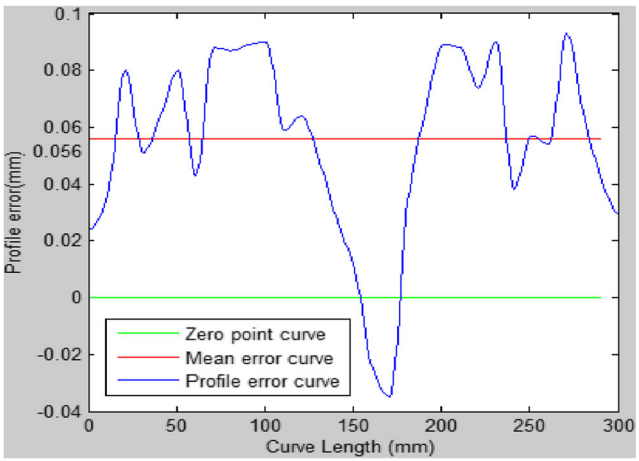

Fig. 7 Precision of profile with no compensation

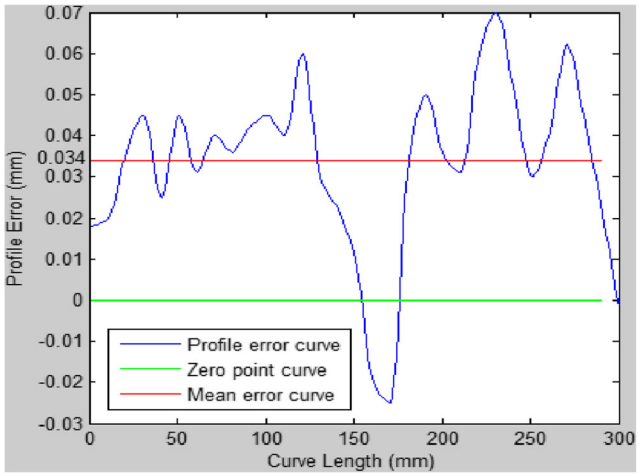

Fig. 8 Precision of profile using only geometric error compensation

3.4 Implementation of error compensation

The value of the error for the different machined points on the tool path is determined based on the developed error model and the measured error data. The G-code compensation is completed after modifying the X, Y, and Z values of the ideal case using the NC program. Because the number of compensated points is large, and therefore a large number of matrices need to be calculated, it is impractical to apply only the artificial calculation. Considering the powerful data processing capability of MATLAB and the interface editing function C#, and then by combining the correlation function of MATLAB and C#, the developed model is generated by the dynamic-link library (DLL) by MATLAB. The DLL can be called directly by Visual Studio 2010. Finally, the comprehensive error compensation is then achieved by using the error compensation software.

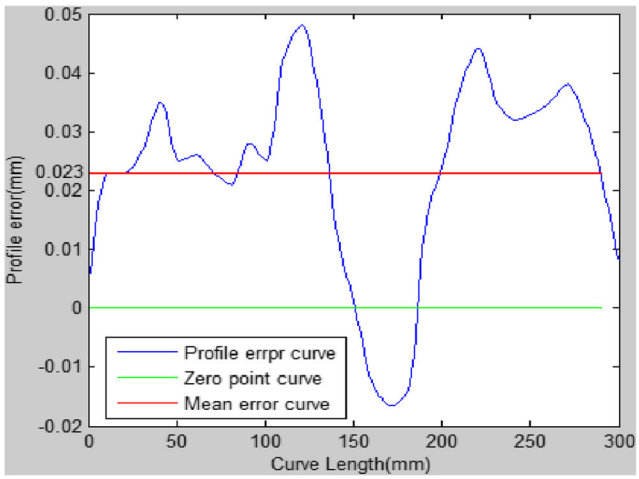

Fig. 9 Precision of profile using comprehensive error compensation

4 Experiments and results

Three groups of experiments were performed to verify the validity of the compensation method. They were used to test the precision of the work-piece profiles, the error compensation protocol of each group being (i) without performing any compensation, (ii) only performing geometric-error compensation, and (iii) performing comprehensive error compensation. The effective validation of geometric error compensation is performed in the no-load state for machine tool and that comprehensive error compensation is performed under conditions where the equivalent cutting force is loaded along the X- and Y-axes. The processed material is 45 steel. The cutting parameter, cutter type, and other experimental factors are mutually consistent.

The work-piece to be processed is shown in Fig. 5. The left slot was milled with no compensation, the center slot while performing only geometric error compensation, and the right slot using comprehensive error compensation. The spatial contour error of the milled slots was measured by the coordinate measuring machine. The measurement test and measurement results are given in Figs. 6, 7, 8, and 9.

Figures 7, 8, and 9 show that the contour error decreases significantly with increasing compensation parameters. The average value of the contour error is 56 μm with no compensation. When geometric-error compensation was used, the profile error is reduced to 34 μm. The precision of the profile has increased 39 % compared with that without compensation. When comprehensive error compensation is implemented, the profile error further decreases to 23 μm. Compared with the other two compensation procedures, the machining accuracy has increased by 59 and 32 %, respectively.

5 Conclusions

A new equivalent cutting-force load-on scheme was established in this paper. The loading scheme of the equivalent cutting force ensures a stable measurement environment for applying laser interferometer. The identification of the comprehensive error parameter becomes much more convenient, and the corresponding relationship between force and error can be directly established using laser interferometer under such conditions. This avoids indirect conversion process when the cutting force error is compensated. This direct measurement method of equivalent-cutting-force induced error provides a novel technical means for studying comprehensive error compensation.

A comprehensive error compensation model was developed based on the theory of multi-body systems and the use of homogeneous coordinate transformations. The unique model was used to compensate both geometric and cutting-force-induced errors simultaneously by a single model. Comprehensive error compensation regarding the geometric and cutting-force-induced errors was performed. To further highlight the usefulness of the compensation method, the comprehensive error compensation was achieved by admixture programming using MATLAB and C#. In practical applications of error compensation, this adds much more flexibility and reliability in industrial production.

The experimental results showed that the precision from the machine tool after performing comprehensive error compensation improved by 59 % with respect to that without compensation. The effectiveness and feasibility of the compensation method were verified in this compensation test. The machine accuracy was improved significantly. Comprehensive error compensation using an equivalent cutting force provides a good theoretical basis to implement a more complete study.

Acknowledgments This research was funded by the National Natural Science Foundation of China (Grant No. 51375100), Guangdong Science and Technology Project (Grant No 2013B011304009) and Outstanding Dissertation Cultivation Project of Guangdong Province (Grant No. 521005006).

References

1. Ramesh R, Mannan MA, Poo AN (2000) Error compensation in machine tools—a review Part I: geometric, cutting-force induced and fixture dependent errors. Int J Mach Tools Manuf 40:1235–1256
2. Rahman M, Heikkala J, Lappalainene K (2000) Modeling measurement and error compensation of multi-axis machine tools. Part I: theory. Int J Mach Tools Manuf 40:1535–1546
3. Liu H, Li B, Wang X, Tan G (2011) Characteristics of and measurement methods for geometric errors in CNC machine tools. Int J Adv Manuf Technol 54:195–201
4. Tian W, Gao W, Zhang D, Huang T (2014) A general approach for error modeling of machine tools. Int J Mach Tools Manuf 79:17–23
5. Zhu S, Ding G, Qin S, Lei J (2012) Integrated geometric error modeling, identification and compensation of CNC machine tools. Int J Mach Tools Manuf 52:24–29
6. Srivastava AK, Veldhuis SC, Elbestawit MA (1995) Modelling geometric and thermal errors in a five-axis CNC machine tool. Int J Mach Tools Manuf 35(9):1321–1337
7. Ahn KG, Cho DW (1999) Proposition for a volumetric error consideration backlash in machine tools. Int J Adv Manuf Technol 15: 554–561
8. Lin Y, Shen Y (2003) Modeling of five-axis machine tool metrology models using the matrix summation approach. Int J Adv Manuf Technol 21:243–248
9. Belforte G, Bona B, Canuto E, Donati F, Ferraris F, Gorini I (2003) Coordinate measuring machines and machine tools self-calibration and error correction. Ann CIRP 36(1):359–364
10. Zuo X, Li B, Yang J, Jiang X (2013) Integrated geometric error compensation of machining processes on CNC machine tool. 14th CIRP Conference on Modeling of Machining Operations 8:135–140
11. Jung J-H, Choi J-P, Lee S-J (2006) Machining accuracy enhancement by compensating for volumetric errors of a machine tool and on-machine measurement. J Mater Process Technol 174:56–66

12. Engin S, Altintas Y (2001) Mechanics and dynamics of general milling cutters, part 1. Helical end mill. Int J Mach Tools Manuf 41:2195–2212
13. Raksiri C, Parnichkun M (2004) Geometric and force errors compensation in a 3-axis CNC milling machine. Int J Mach Tools Manuf 44:1283–1291
14. Ratchev S, Liu S, Huang W, Becher AA (2006) An advanced FEA based force induced error compensation strategy in milling. Int J Mach Tools Manuf 46:542–551
15. Yang Y, Li X, Liang G, Shao X (2013) A new approach for predicting and collaborative evaluating the cutting force in face milling based on gene expression programming. J Netw Comput Appl 36:1540–155
16. Schmitz TL, Ziegert JC, Canning JS, Zapata R (2008) Case study: a comparison of error sources in high-speed milling. Precis Eng 32: 126–133
17. Ikua BW, Tanaka H, Obata F, Sakamoto S (2001) Prediction of cutting forces and machining error in ball end milling of curved surfaces I: theoretical analysis. Issue Ser Title: Precis Eng 25:266–273
18. Chen Z (2008) Real-time compensation of cutting-force-induced error on CNC machine tools [D]. Shanghai Jiao Tong University (China)